Ultrastructural Alterations in Liver of Mice Exposed Chronically and Transgenerationally to Aqueous Extract of Betel Nut: Implications in Betel Nut-Induced Carcinogenesis

YASHMIN CHOUDHURY AND RAJESHWAR N. SHARAN*
Department of Biochemistry, Radiation and Molecular Biology Unit, North-Eastern Hill University, Shillong 793022, India

KEY WORDS betel nut; transgenerational exposure; mitochondrial index; predisposition to cancer

ABSTRACT The aqueous extract of betel nut (AEBN) induces the formation of preneoplastic nodules in the liver of Swiss Albino mice and leads to increased predisposition to cancer when administered transgenerationally. The aim of this investigation was to elucidate the alterations in ultrastructure of subcellular organelles in the liver nodules using transmission electron microscopy and to determine whether these alterations have implications in AEBN-induced carcinogenesis. Male and female Swiss Albino mice were exposed to AEBN chronically and transgenerationally at a dose of 2 mg/mL in drinking water for 24 weeks. Extensive polymorphism was noted in nuclear shape and heterochromatin organization. Heterochromatin aggregation and marginalization were observed in the nuclei of chronically exposed mice, whereas transgenerationally exposed mice exhibited dispersion or loss of heterochromatin. The nuclear envelope was disrupted, and the nucleoli were enlarged in chronically exposed mice, whereas in transgenerationally exposed mice the nucleoli were reduced in size or totally absent. The cisternae of the rough endoplasmic reticulum were dilated and disrupted, and a large number of autophagic vesicles were observed in both chronically and transgenerationally exposed mice. Atypical mitochondria that underwent extensive cristolysis and progressively declined in size and number from the chronically exposed mice to the different generations of transgenerationally exposed mice were also observed. Thus, exposure to AEBN resulted in severe loss of ultrastructural integrity of cells in the liver nodules, and the progressive loss of mitochondrial function appeared to play a significant role in increasing the predisposition to cancer of mice exposed transgenerationally to AEBN. *Microsc. Res. Tech. 00:000–000, 2009.*

INTRODUCTION

The structural and functional integrity of subcellular organelles is of paramount importance in the maintenance of a normal cell. A cancer cell departs from the functions of a normal cell and may also be expected to exhibit wide variations in structure. In fact, various reports have enumerated the structural alterations in organelles, observed in different kinds of cancer (Merkow et al., 1967; Raick, 1973; Zhang and Takenaka, 1995; Arismendi-Morillo and Castellano-Ramirez, 2008; Caruso et al., 2008). It, thus, emerges that carcinogenesis is associated with some characteristic alterations in the structure and functions of subcellular organelles.

Betel nut (BN) is a common carcinogen to which a large population across the world is exposed (Sharan, 1996). At cellular and molecular levels, BN extract was found to decrease the cell survival, vital dye accumulation, and membrane integrity of cultured human buccal epithelial cells and to induce formation of both DNA single strand breaks and DNA-protein cross links (Sundqvist et al., 1989). Ripe BN extract induced significant decline in population doubling, increase in senescence, cell-cycle arrest at G_1/S phase, and decrease in cell proliferation of cultured normal human oral keratinocytes (Lu et al., 2006), and an aqueous extract of BN (AEBN) induced DNA-strand breaks and enhanced cell proliferation of mouse kidney cells in vitro (Wary and Sharan, 1988). Exposure of Swiss Albino mice to AEBN has also been reported to induce formation of preneoplastic nodules of the liver (Sharan, 1996). Thus, Swiss Albino mice exposed to AEBN serves as a good model for the study of BN-induced carcinogenesis. Using this model, we have previously characterized the alterations in p53 response associated with the different stages of AEBN-induced carcinogenesis in mice and, also, reported that transgenerational exposure of mice to AEBN resulted in an increased predisposition to cancer (Choudhury and Sharan, 2009). To extend the study to the structural level, we performed histological examination of the liver nodules of P generation mice exposed chronically to AEBN and their transgenerationally exposed F1,

*Correspondence to: Dr. R.N. Sharan, Department of Biochemistry, North-Eastern Hill University, Umshing, Shillong 793 022, India.
E-mail: rnsharan@nehu.ac.in

Received 10 August 2009; accepted in revised form 15 September 2009
DOI 10.1002/jemt.20791
Published online in Wiley InterScience (www.interscience.wiley.com).

F2, and F3 offspring by hematoxylin and eosin staining. The corresponding regions of livers of age-matched control mice not exposed to AEBN were also examined histologically. The hematoxylin and eosin stained sections of liver nodules exhibited a number of alterations in comparison with the corresponding regions of normal liver (Choudhury and Sharan, 2009). In liver of control mice, the cells were uniformly shaped and were closely attached with one another in a regular arrangement. In contrast, the cells of liver nodules developing in P generation mice after 16 weeks, in F1 mice after 8 weeks, F2 mice after 6 weeks, and F3 mice after 4 weeks of exposure to AEBN were distorted in shape, had enlarged nuclei, and also displayed loss of attachment from neighboring cells, which are features of transformed cells, confirming that the nodules were preneoplastic. Histological examination of the well-developed liver nodules after 24 weeks of exposure revealed irregularly shaped cells with enlarged nuclei and more pronounced loss of attachment, exhibiting a trabecular pattern, which is a characteristic feature of hepatocellular carcinoma (Narama et al., 2003). The incidence of preneoplastic nodule formation in the liver was 100% in the P as well as F1 through F3 generation mice. The numbers of nodules that developed per liver were determined to be 1.4 ± 0.5 in P generation mice, 3.08 ± 0.76 in F1 mice, 3.33 ± 0.76 in F2 mice, and 3.53 ± 0.52 in F3 mice, after 24 weeks of exposure to AEBN. However, this increase in frequency of nodulation was not found to be significant using the χ^2 test with Yates' correction. No sex-associated difference was observed in the frequency of nodule development (Choudhury and Sharan, 2009). No nodule development was observed in the liver of the control mice throughout the duration of the experiments. Thus, the predisposition to cancer of AEBN-exposed mice was largely manifested by the advancement in the period of appearance of preneoplastic nodules of the liver. Because a correlation was observed between the period of appearance of preneoplastic nodules and structural alterations at light microscopic level as revealed by hematoxylin and eosin staining (Choudhury and Sharan, 2009), it was of interest to elucidate the alterations in subcellular organelle structure induced by AEBN at electron microscopic level and to determine if these alterations were, in any way, associated with carcinogenic risk induced by transgenerational exposure to AEBN.

MATERIALS AND METHODS

Animals

Six-week-old inbred Swiss Albino mice (25 ± 1 g) were used in this study. They were housed in polycarbonate cages with husk bedding in a well-ventilated animal room maintained at 25°C. Standard mouse pellet and drinking water with or without AEBN were provided ad libitum. The mice were maintained in groups of four to five mice per cage for each data point. Each experiment was repeated at least thrice, that is, the total number of mice per data point was 15 ± 1. The ratio of male to female mice was $7 \pm 1/8 \pm 1$. All experiments were conducted according to the guidelines of the Institutional Ethics Committee for animal experimentation.

AEBN Exposure Protocol and Experimental Design

AEBN was prepared as described earlier (Wary and Sharan, 1988) and administered at a dose of 2 mg/mL in drinking water in chronic and transgenerational exposure regimes, as reported previously (Choudhury and Sharan, 2009). It has been estimated that each mouse, on an average, consumed ~7 mL of drinking water per day. Thus, each AEBN-exposed mouse must have accumulated ~14 mg of AEBN per day.

Chronic Exposure

Six-week-old male and female mice were given AEBN in drinking water ad libitum up to 24 weeks. These mice have henceforth been referred to as the previously unexposed (P) generation mice. Age-matched mice provided drinking water without AEBN served as controls.

Transgenerational Exposure

Male and female mice of the P generation exposed to AEBN in drinking water for 6 weeks were allowed to breed by maintaining one male and four female mice per cage with standard food pellet and drinking water containing AEBN ad libitum. The offspring of the exposed P generation mice constituted the F1 generation exposed mice. Postweaning, that is, at 6 weeks of age, the F1 mice were separated from their parents, male and female mice being maintained separately and were exposed to AEBN in drinking water. Male and female F1 mice exposed to AEBN for 6 weeks were also allowed to breed the same way to raise the F2 generation, and the F3 generation was similarly raised from the F2 generation mice exposed to AEBN for 6 weeks. Six weeks old male and female F1, F2, and F3 mice were also exposed to AEBN as the P generation mice for a period up to 24 weeks. Age-matched, unexposed control mice of the P generation were also allowed to breed in parallel, and their offspring served as age-matched controls for the F1, F2, and F3 exposed mice, respectively.

The mice exposed chronically and transgenerationally to AEBN were monitored carefully throughout the period of treatment for any visible alteration or sign of ill-health. P, F1, F2, and F3 generation mice as well as their respective age-matched controls were sacrificed at regular intervals for the investigation.

Transmission Electron Microscope Studies

As done for hematoxylin and eosin stained histological slides (Choudhury and Sharan, 2009), regions of nodules in the livers of P, F1, F2, and F3 mice exposed to AEBN for 24 weeks, and the corresponding regions of the livers of age-matched control mice were examined using 100 CXII JEOL transmission electron microscope at the Sophisticated Analytical Instrumentation Facility, North-Eastern Hill University, Shillong. Samples were prepared following the standard protocol described by Hayat (1985), with minor modifications. Briefly, liver was cut into 1-mm thick pieces and fixed in Karnovsky's fixative for 4 h. They were washed thrice by immersion in 0.1 M cacodylate buffer for 10 min, followed by centrifugation at 10,000*g* for

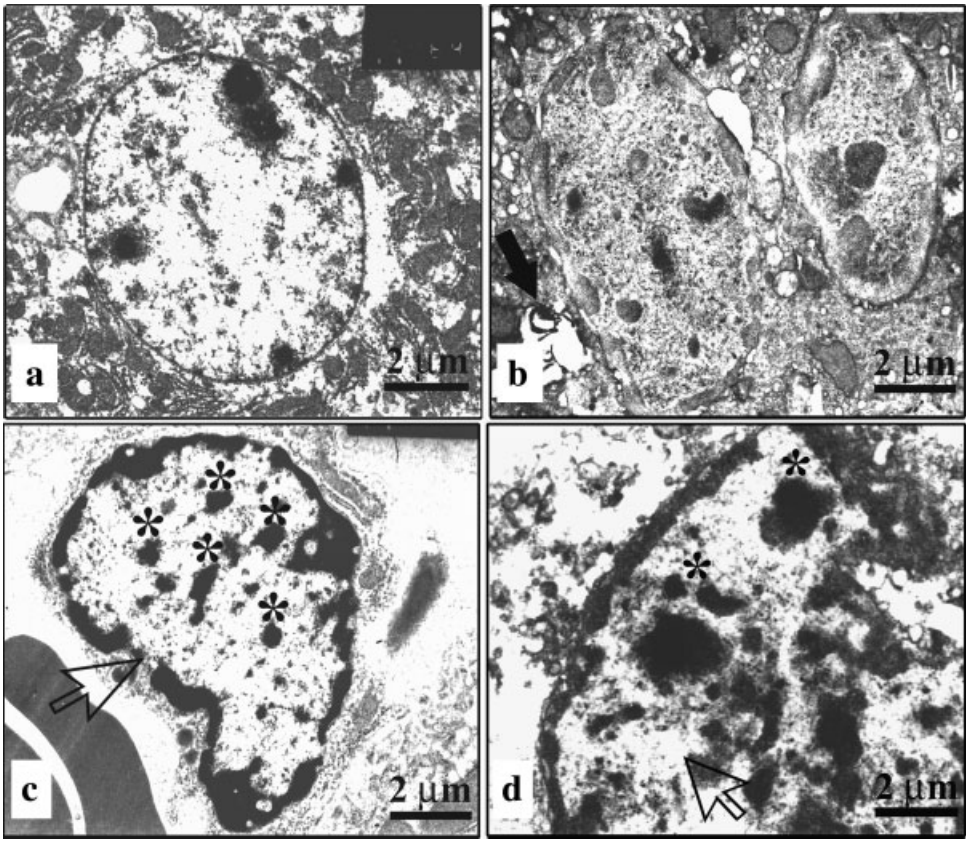

Fig. 1. Alterations in the nucleus in liver nodules of mice exposed chronically to AEBN in comparison with control mice. **a**: Nucleus of hepatocyte of control mouse is ellipsoidal in shape with intact nuclear envelope and distinct nucleoli; **b**: binucleate hepatocyte in liver nodule of chronically exposed P generation mouse with deformed nuclei; closed arrow indicates autophagic vesicle; **c**: nucleus with altered shape, coarse heterochromatin aggregates (asterisk) and disrupted nuclear envelope (open arrow) in hepatocyte of liver nodule of chronically exposed P generation mouse; **d**: nucleus with disrupted nuclear envelope (open arrow) and coarse heterochromatin aggregates (asterisk) in hepatocyte of liver nodule of a chronically exposed P generation mouse.

1 min. Post-fixation was performed in 1% OsO_4 for 1 h, followed by clearing in propylene oxide with 2 changes for 30 min each at room temperature (RT). The pieces were embedded sequentially in a mixture of embedding medium and propylene oxide in the ratio 1:3, overnight at RT, in the ratio 1:1 for 1 h at RT and in the ratio 3:1 for 1 h at RT. They were kept for 1 h in vacuum and then transferred to pure embedding medium at 50°C. Finally, the pieces were placed in embedding capsules (Better Equipment for Electron Microscopy, NY), covered with pure embedding medium, and left at 50°C for 12 h. Sections 60- to 90-nm were cut with the help of an ultramicrotome. The sections were stained with uranyl acetate for 30–120 min at RT, as described by Terzakis (1968), and viewed and photographed at different magnifications ranging from 5000× to 40,000×.

Statistical Analysis

The data pertaining to total number of mitochondria per micrograph and total area of mitochondria per micrograph is the mean ± SD of at least 3 independent experiments for each generation of mice. The significance of decline in mitochondrial index of P, F1, F2, and F3 mice with respect to control has been determined using Student's *t*-test.

RESULTS

General and Histological Observations

As previously reported (Choudhury and Sharan, 2009), mice exposed chronically to AEBN were found to develop liver nodules primarily in the right and caudate lobes of the liver after 16 weeks of exposure to AEBN. The appearance of the nodules was significantly accelerated and advanced in mice exposed transgenerationally to AEBN. They appeared after 8 weeks of exposure in F1 mice, 6 weeks of exposure in F2 mice, and 4 weeks of exposure in F3 mice. These nodules were confirmed to be preneoplastic by histological examination as described recently (Choudhury and Sharan, 2009).

Transmission Electron Microscope Studies

Extensive alterations were observed in the ultrastructure of hepatocytes of liver nodules developing in P, F1, F2, and F3 mice after 24 weeks of exposure to AEBN in comparison with the hepatocytes of corresponding regions of the liver of age-matched control mice.

Alterations in Ultrastructure of the Nucleus

The nucleus of control mice was spherical in shape with an intact double-layered nuclear envelope and well-defined nucleoli (Fig. 1a). In contrast, the liver nodules of chronically exposed mice revealed pleomorphism of the nucleus. Most cells were observed to be binucleate (Fig. 1b). Moreover, the nuclei assumed varied shapes and sizes (Figs. 1b–1d, 2a, and 2b), with marked chromatin marginalization (Figs. 1c, 1d, 2a, and 2b). Disruption of the nuclear envelope was also observed (Figs. 1c and 1d; open arrow). Nuclei of chronically exposed mice exhibited atypical nucleoli: the nucleoli were enlarged (Figs. 2a and 2b) and appeared to be distinctly demarcated from a region surrounding them, which is possibly condensed chromatin, and is made up of electron-dense as well as comparatively electron-sparse areas (Figs. 2a and 2b; inset). Extensive disruptions of normal nuclear structure were also observed in the liver nodules of transgenerationally exposed mice (Fig. 3). These comprised altered shape (Figs. 3a, 3b, and 3d), loss of heterochromatin (Figs. 3a, 3b, and 3d), dispersion of heterochromatin (Fig. 3c), disruption of nuclear envelope (Figs. 3a, b, and 3d; open arrow), and presence of inconspicuous nucleoli (Figs. 3a, 3b, and 3d) or total absence of nucleoli (Fig. 3c).

Alterations in Ultrastructure of the Rough Endoplasmic Reticulum

The rough endoplasmic reticulum (RER) of control mice was an extensive, well-stacked system of cisternae, with ribosomes attached to the surface of the membrane appearing as electron-dense particles (Fig. 4a). However, the cisternae of the RER of chronically exposed P generation mice were dilated and less extensive and were disrupted at several places (Fig. 4b). The disruption of the RER cisternae is clearly evident at higher magnification (Fig. 4c). The RER of the transgenerationally exposed mice exhibited poorly stacked, much sparse, and dilated cisternae than those of chronically exposed mice (Figs. 5a–5c; open arrows).

Alterations in Ultrastructure of Mitochondria and Mitochondrial Index

The liver of control mice had a large number of mitochondria of varying shapes and sizes (Fig. 6a). However, the mitochondria in the liver of chronically exposed mice were smaller in size than in the control mice (Fig. 6b). The mitochondria in the liver of the transgenerationally exposed mice appeared to be rounded in shape and were significantly fewer in number and smaller in size than in the control (Figs. 6c–6e). At higher magnification (Fig. 7), the mitochondria of the control mice showed a double-layered membrane, which was convulated to form an extensive array of cristae (Fig. 7a). The mitochondria of the chronically exposed mice, however, exhibited disarrangements of cristae and cristolysis (Fig. 7b; arrow). The mitochondria of the transgenerationally exposed mice were swollen and rounded. They also declined progressively in size from the F1 through the F3 generation and displayed extensive cristolysis (Figs. 7c–7e). The total number of mitochondria per micrograph was determined to be 17 ± 1.5 in control mice, 24 ± 0.7 in P generation mice, 6.33 ± 0.58 in F1 mice, 5.67 ± 0.58 in F2 mice, and 3.67 ± 0.47 in F3 mice. The total area of mitochondria per micrograph were determined to be 3.07 ± 1 μm^2 in control mice, 1.8 ± 1.1 μm^2 in P generation mice, 1.76 ± 0.9 μm^2 in F1 mice, 0.65 ± 0.32 μm^2 in F2 generation mice, and 0.41 ± 0.24 μm^2 in F3 mice. The mitochondrial index (the product of the total number and total area of mitochondria per micrograph) was calculated as an indicator of mitochondrial function. It was found to decrease progressively from the P through F3 generations in comparison with the control, with significant decline observed from F1 through F3 generations (Fig. 8).

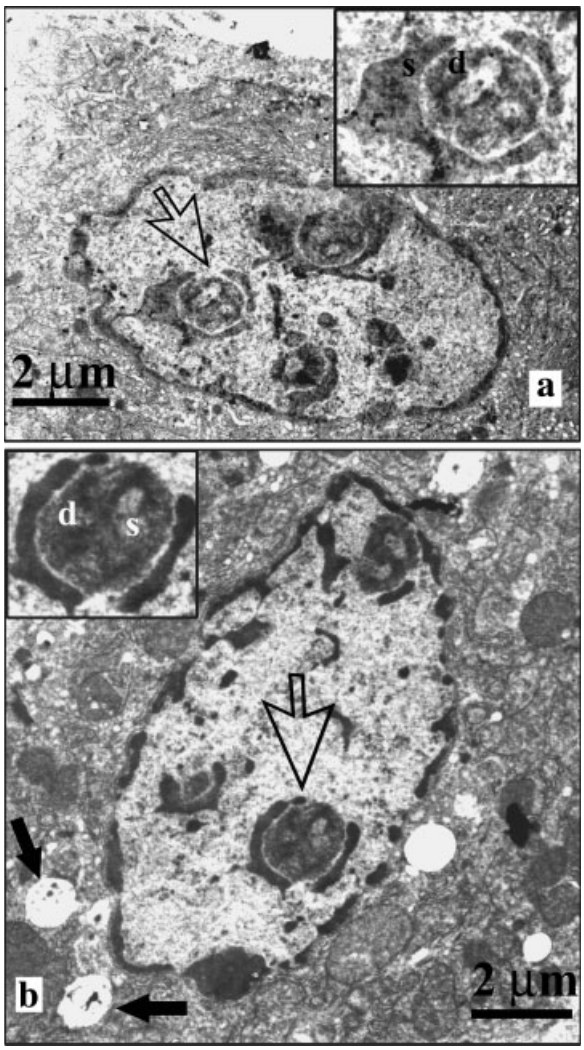

Fig. 2. Changes in the nucleoli of mice exposed to AEBN. **a**: Enlargement of nucleoli in the nuclei of mice exposed chronically to AEBN (open arrows). Inset: each nucleolus is apparently demarcated from a surrounding layer of condensed chromatin and comprises electron-dense (d) and electron-sparse (s) regions; **b**: closed arrows show autophagic vesicles.

In addition to the above observed alterations, micrographs of both chronically and transgenerationally exposed specimens revealed various electron-lucent bodies of varying shape and size enclosed by a double-layered membrane (Figs. 1b, 2b, 3a–3d, and 5a–5c; closed arrows), some of which enclosed fragments of

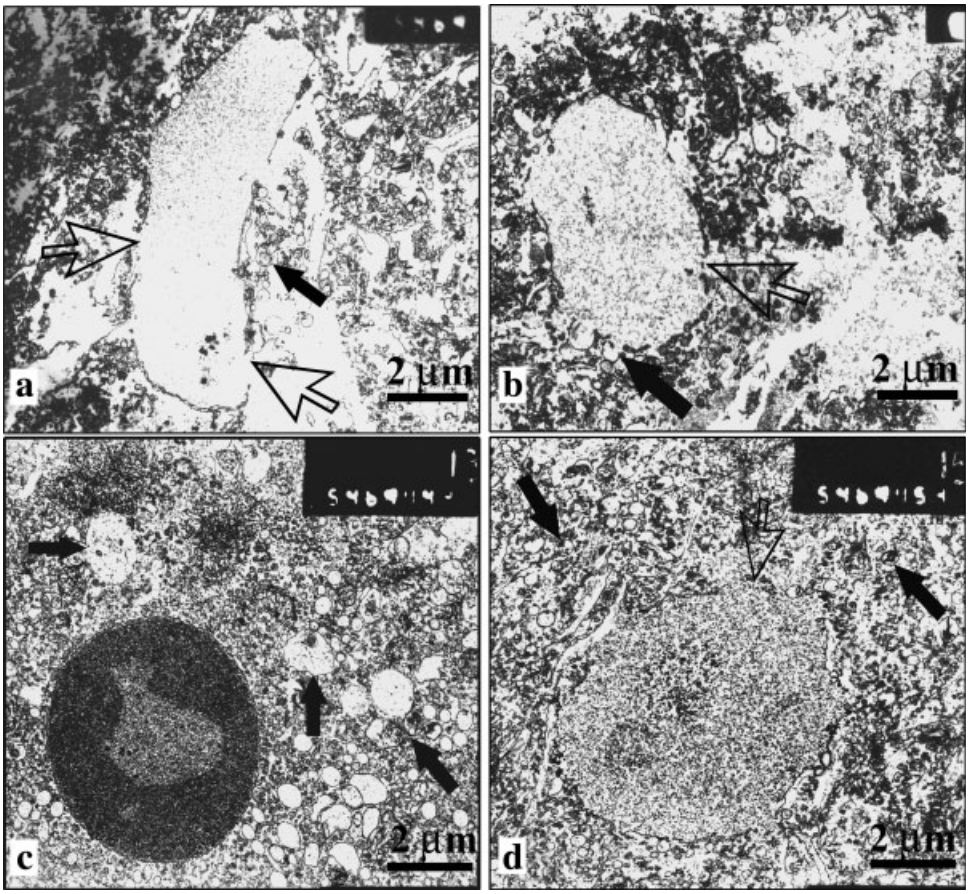

Fig. 3. Alterations in the nucleus in liver nodules of mice exposed transgenerationally to AEBN. **a**: Nucleus of hepatocyte of F1 mouse is altered in shape with disrupted nuclear envelope (open arrows), loss of heterochromatin, and inconspicuous nucleoli; closed arrow indicates autophagic vesicles; **b**: nucleus of hepatocyte of F2 mouse is altered in shape with disrupted nuclear envelope (open arrow), loss of heterochromatin, and inconspicuous nucleoli; closed arrow indicates autophagic vesicles; **c**: nucleus of hepatocyte of F3 mouse with dispersed heterochromatin and absence of nucleoli; closed arrows show autophagic vesicles; **d**: nucleus of hepatocyte of F3 mouse is altered in shape with disrupted nuclear envelope (open arrow), loss of heterochromatin, and inconspicuous nucleoli; closed arrows indicate autophagic vesicles.

subcellular organelles (Figs. 1b, 2b, 3c–3d, 5a–5c; closed arrows) and were identified as autophagic vesicles. These vesicles were not observed in the hepatocytes of control mice.

DISCUSSION

The alterations in nuclear size and shape, in numbers and sizes of nucleoli, and in chromatin texture are characteristic of a given tumor type and stage and are used in cancer diagnosis. They might also be related to the altered functional properties of cancer cells (Zink et al., 2004). This study reveals that exposure to AEBN induces extensive alterations in the ultrastructure of the nucleus (Figs. 1–3), exhibiting a wide gamut of changes, all of which have been reported to be associated with different types of precancerous lesions and cancer (Zink et al., 2004). The most persistent nuclear alterations observed were changes in nuclear shape and heterochromatin organization (Figs. 1–3). The nuclear lamina, which is the layer immediately beneath the nuclear envelope, is thought to be a principal determinant of nuclear shape. Many chromatin attachment points lie at the inner surface of the nuclear lamina. In most cell types, this peripheral layer of chromatin is transcriptionally silent, and its association with heterochromatin seems to be involved in transcriptional repression of gene loci. Alterations of nuclear shape are often associated with altered organization of heterochromatin or loss of heterochromatin aggregates (Zink et al., 2004), as also observed in this study (Figs. 1a, 1b, 3a, 3b, and 3d). It is possible that changes in the nuclear lamina and nuclear shape affect chromatin organization and gene positioning, respectively, and, in this way, alter patterns of gene expression, contributing to transformation (Zink et al., 2004). Changes in chromatin texture are also frequently observed in cancer cells (Zink et al., 2004). These are probably caused by either condensation or decondensation of chromatin domains resulting in "chromatin coarsening" or "open chromatin," which correspond to an increase or loss of heterochromatin aggregates, respectively, as observed in this study (Figs. 1c, 1d, and 3c; Figs. 3a, 3b, and 3d, respectively). Changes in chromatin texture have been shown to be associated with

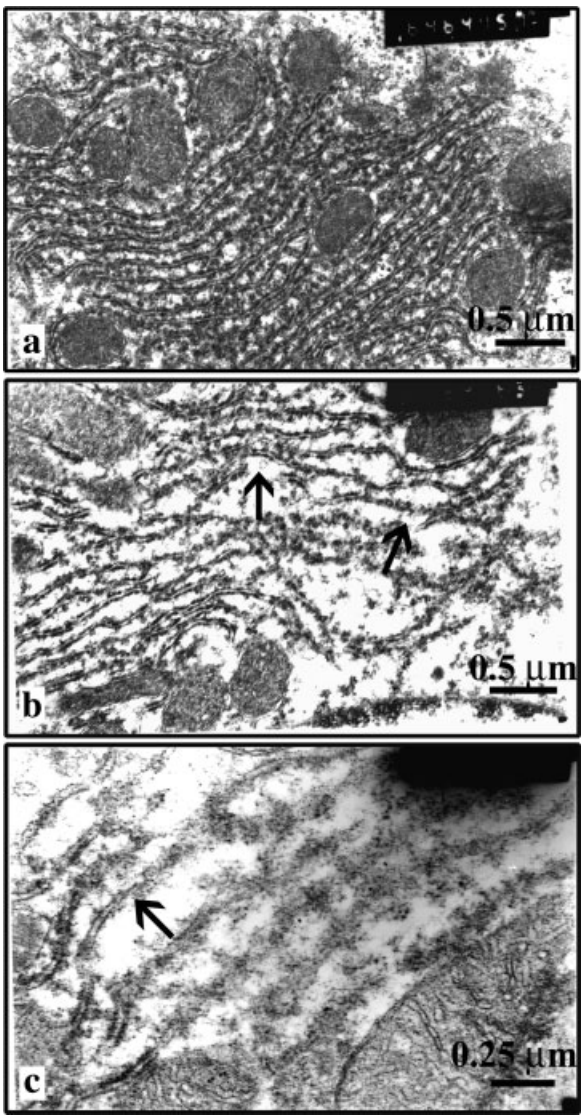

Fig. 4. Alterations in the RER of liver nodules of mice exposed chronically to AEBN in comparison with control. **a**: RER of hepatocytes of control mice with well-stacked cisternae; the ribosomes attached to the surface appear as electron-dense particles; **b**: RER of hepatocytes in liver nodules with dispersed and poorly stacked cisternae, disrupted at several places (arrows); **c**: RER of hepatocytes in liver nodules at higher magnification showing disrupted cisternae (arrow).

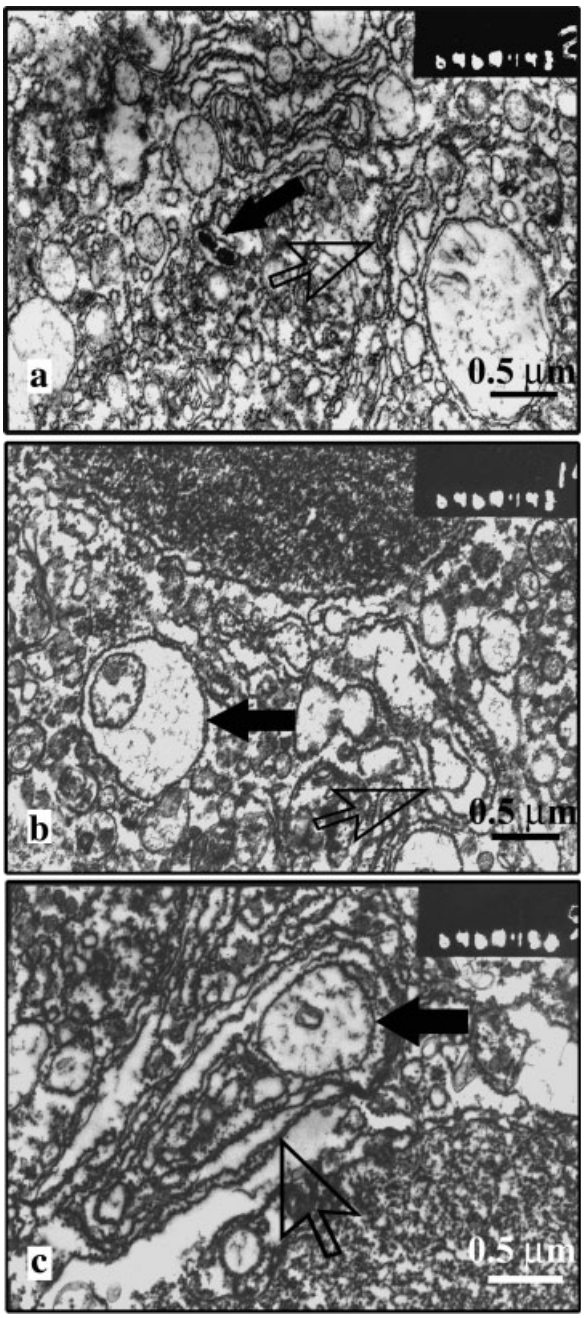

Fig. 5. Alterations in the RER of liver nodules of mice exposed transgenerationally to AEBN, RER of hepatocytes of in liver nodules of F1 (**a**), F2 (**b**), and F3 (**c**) mice, respectively, showing poorly stacked cisternae with attached ribosomes appearing as electron-dense particles (open arrows). Closed arrows indicate autophagic vesicles.

changes in gene expression patterns and seem to be important for oncogene-dependent tumorigenesis, as well as for tumor-suppressor-dependent antitumor mechanisms (Zink et al., 2004). It is likely that the changes in chromatin texture observed in this study are associated with alterations in the p53 tumor suppressor response, as previously reported (Choudhury and Sharan, 2009). Another nuclear component that is frequently altered in tumor cells is the nucleolus, with the nucleoli becoming more prominent in many types of cancer cells (Zink et al., 2004). Chronic exposure to AEBN was found to cause enlargement of the nucleolus (Figs. 2a and 2b; inset), whereas transgenerational exposure resulted in the formation of inconspicuous nucleoli (Fig. 3a, 3b, and 3d) and total absence of nucleoli (Fig. 3c). Nucleolar size is typically assumed to reflect the rate of ribosome production (Zink et al., 2004), and one possible explanation for the observed nucleolar enlargement upon chronic exposure to AEBN would be to maintain a high level of ribosome production required to sustain the increased cellular

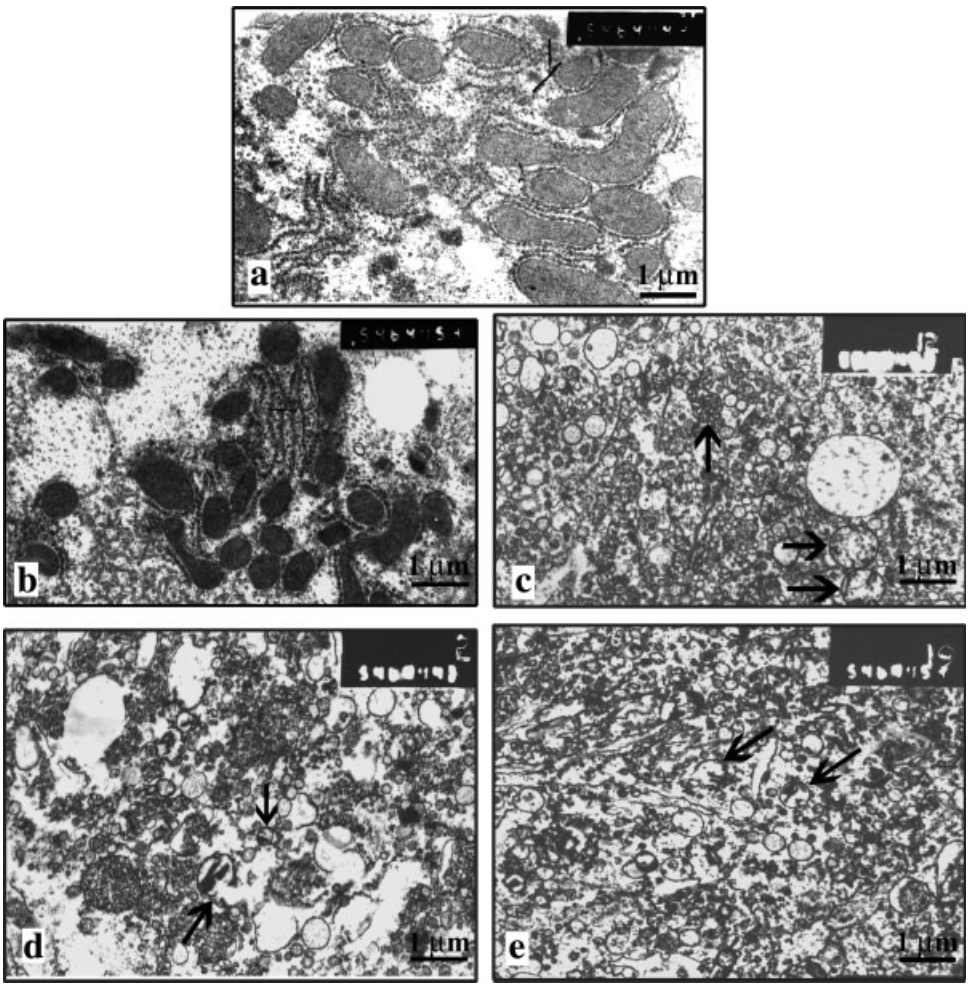

Fig. 6. Decline in number of mitochondria in mice exposed chronically and transgenerationally to AEBN in comparison with control. **a**: Mitochondria in hepatocytes of control mice; **b**: mitochondria in liver nodules of chronically exposed F1 mice were fewer in number than in control; mitochondria in liver nodules of transgenerationally exposed F1 mice (**c**) F2 mice (**d**), and F3 mice (**e**) were fewer in number and smaller in comparison with control (arrows). It may be noted that the mitochondria also decline progressively in size from the P through F3 generation in mice.

proliferation leading to the formation of liver nodules. However, the nucleolar changes might also be related to other nucleolar functions, such as mRNA transport, p53 metabolism, and the control of cell proliferation (Zink et al., 2004), and the decrease in size or absence of nucleoli on transgenerational exposure to AEBN might result in a gross reduction or loss of these vital functions.

The ER is responsible for the synthesis, initial post-translational modification, proper folding, and maturation of newly synthesized transmembrane and secretory proteins and, also, functions as a regulator of intracellular homeostasis (Shiraishi et al., 2006). Arecoline, the major alkaloid of BN, has been reported to cause disruptions in hepatocyte ultrastructure in mice, including profuse inflation of the RER cisternae (Dasgupta et al., 2006). Arecoline has also been reported to cause suppression of the activity of the pineal gland in rats by inducing various ultrastructural alterations, such as dilation of the cisternae of the RER (Saha et al., 2007). Our studies reveal reduced stacking and dilation of the RER cisternae in the liver nodules of mice exposed both chronically (Fig. 4b) and transgenerationally (Figs. 5a–5c) to AEBN. The degree of dilation of the cisternae was observed to be greater in transgenerationally exposed F1, F2, and F3 mice (Figs. 5a–5c) in comparison with the chronically exposed P generation mice. It is, thus, likely that the observed aberration in RER structure induced by AEBN-exposure is mediated by arecoline (Dasgupta et al., 2006; Saha et al., 2007). This disruption of normal RER structure may be one of the factors contributing toward the detrimental effect of AEBN on mice.

Mitochondria are the powerhouse of the cell. They play a vital role in energy metabolism and regulate calcium flux and apoptosis. Cancer cells have an altered metabolism, and mitochondria are directly or indirectly involved in this process. The mitochondria of rapidly growing tumor cells have been reported to be fewer in number, smaller in size, and have poorly organized cristae in comparison with normal and slowly growing

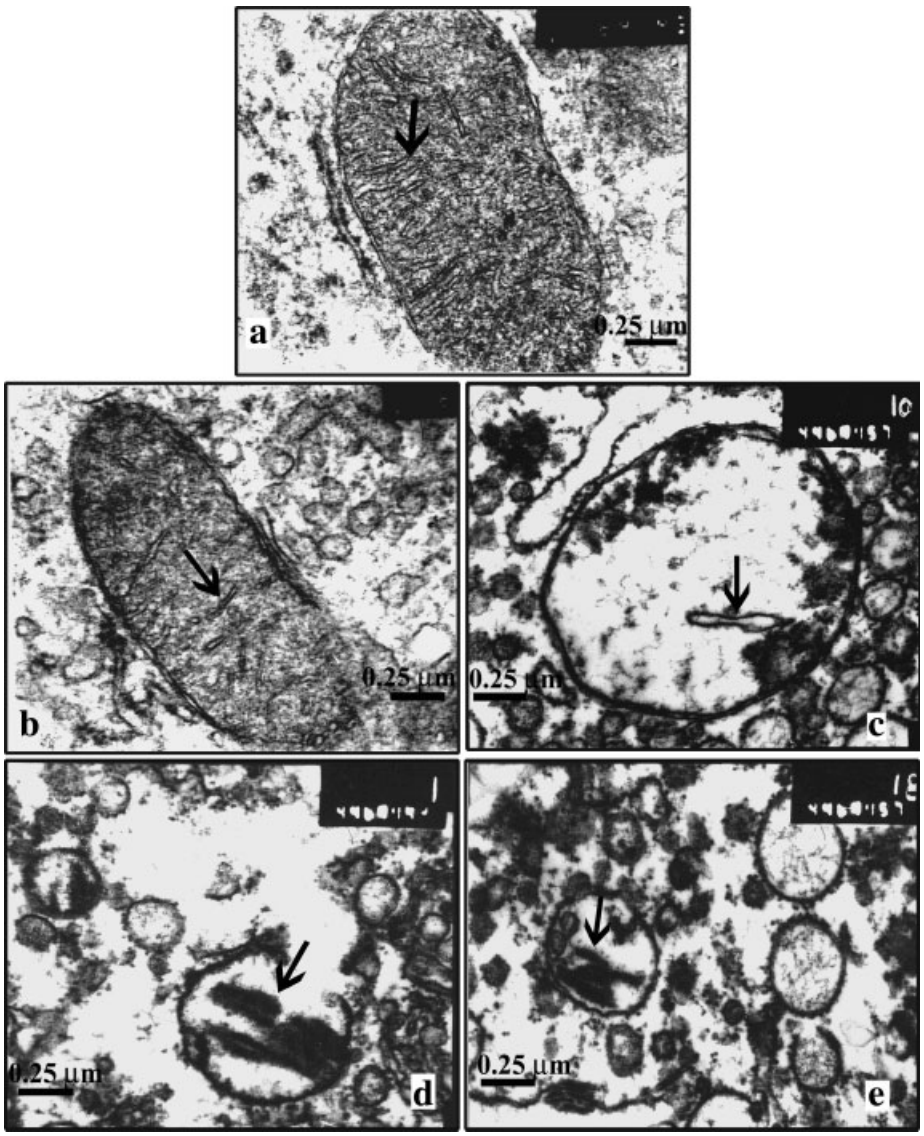

Fig. 7. Alterations in the size and shape of mitochondria in mice exposed chronically and transgenerationally to AEBN in comparison with control. Alterations in the structural integrity of cristae (arrows) were also observed. **a**: Mitochondria of hepatocytes of control mice were tubular in shape with abundant cristae arranged perpendicular to the longitudinal axis of the mitochondrion; **b**: mitochondria of hepatocytes of liver nodules in chronically exposed P mice remained tubular in shape but exhibited disarrangement of cristae and cristolysis; **c**: mitochondria in F1 mice were rounded in shape and exhibited cristolysis; **d**: F2 mice exhibited rounded mitochondria with fewer cristae and smaller size than that of F1 mice. **e**: F3 mice exhibited rounded mitochondria with disarrangement of cristae and were smaller in size than the mitochondria in F1 and F2 mice.

tumors (Paul and Mukhopadhyay, 2007). Diminished mitochondrial numbers have also been reported in rat hepatic tumor cells (Luciakova and Kuzela, 1992). In this study, transgenerational exposure to AEBN was found to induce a progressive decline in the number of mitochondria in the liver of F1 through F3 generation mice, in comparison with control (Figs. 6a, 6c–6e). The normal mitochondrial architecture (Fig. 7a) was severely compromised in chronically exposed mice, with extensive cristolysis being observed (Fig. 7b). Mitochondrial swelling associated with extensive cristolysis was observed in the transgenerationally exposed F1, F2, and F3 mice (Figs. 7c–7e). Similar ultrastructural finding has been reported earlier in case of human astrocytic tumors (Arismendi-Morillo and Castellano-Ramirez, 2008). The mitochondrial index, determined in this study as an indicator of mitochondrial function, was found to decline progressively from the P through F3 generations in comparison with control (Fig. 8). In addition, a previous study reports that the cristae of mitochondria are the prime location of oxidative phosphorylation required for ATP-synthesis (Gilkerson et al., 2003). Therefore, the cristolysis observed in this study suggests that AEBN exposure results in compromised production of ATP by oxidative phosphorylation, which would consequently limit apo-

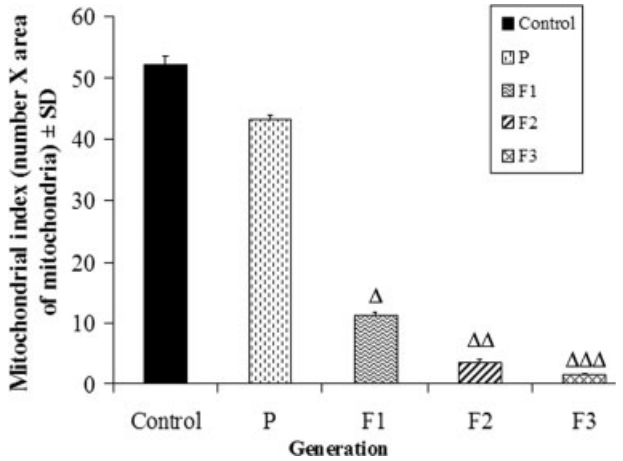

Fig. 8. Bar diagram showing progressive decline in mitochondrial index from P through F3 generation mice in comparison with control. Δ: Significant decline at $P < 0.05$, ΔΔ, at $P < 0.01$, and ΔΔΔ, at $P < 0.001$.

ptosis, because apoptosis is an energy requiring process involving a number of ATP-dependent steps (Zamaraeva et al., 2005). Thus, chronic and transgenerational exposure to AEBN resulted in severe mitochondrial dysfunction, including loss of apoptosis, which increases progressively from the P through F3 generations. This finding is consistent with a previous report that BN extract, and its major alkaloid arecoline induced the cell-cycle arrest but not apoptosis of cultured oral epithelial cells (Chang et al., 2001). It is, therefore, likely that BN and its constituents promoted carcinogenesis by preventing the apoptosis of cells that have incurred DNA damage (Wary and Sharan, 1988; Sundqvist et al., 1989). This would result in an increased susceptibility to cancer in mice exposed transgenerationally to AEBN, thereby accounting for the accelerated appearance of preneoplastic nodules observed in the transgenerationally exposed mice, when they were challenged by the same dose of AEBN as the P generation mice (Choudhury and Sharan, 2009).

All sections of the liver nodules of chronically and transgenerationally exposed mice studied exhibited an abundance of membrane-bound, well-defined bodies of varying size and shape, many of which enclose remnants of cellular debris such as parts of organelles (Figs. 1b, 2b, 3a–3d, and 5a–5c; closed arrows). These bodies are identified as autophagic vesicles, also called autophagosomes (Boya et al., 2005). Autophagy is a regulated process of degradation and recycling of cellular constituents, participating in organelle turnover and in the bioenergetic management of starvation (Boya et al., 2005). A superfluity of these vesicles indicates an increase in autophagy in the liver nodules of AEBN-exposed mice. On starvation, autophagy is greatly increased, allowing the cell to degrade proteins and organelles and, thus, obtain a source of macromolecular precursors, such as amino acids, fatty acids, and nucleotides, which would not be available otherwise (Hippert et al., 2006). Tumors commonly undergo metabolic stress that results in the induction of autophagy in cells possessing an apoptotic defect, thereby supporting their survival (Degenhardt et al., 2006). Thus, autophagy in such cells may be beneficial as a buffer to short-term interruptions in nutrient availability (Degenhardt et al., 2006), and increased autophagy may be expected to promote the growth of solid tumors (Hippert et al., 2006). On exposure to AEBN, cristolysis was found to induce deficiency of oxidative ATP-production and apoptosis. The cells would, therefore, meet their nutritional requirements through autophagy, thus surviving and proliferating in the face of metabolic stress. Such proliferation would allow the formation of liver nodules in AEBN-exposed mice.

Previous studies have shown that, following the exposure of germ cells to a mutagen or carcinogen, an initiating event could be inherited by subsequent generations and revealed after postnatal exposure to mutagens, carcinogens, or nongenotoxic agents (Nomura, 1982, 1983; Tomatis et al., 1992). We have previously reported that, because AEBN is a general carcinogen capable of affecting various tissues, it is likely that exposure of P generation parental mice induces alterations in their germ cells, including alterations in the p53 (Choudhury and Sharan, 2009), and Brca1 and Brca2 responses (unpublished). Moreover, the P generation mice were exposed to AEBN for 6 weeks before mating to raise the F1 mice. Thus, AEBN-induced carcinogenesis would have been initiated during the 6 weeks of exposure before mating (Wary and Sharan, 1988; Choudhury and Sharan, 2009), and the initiating event could be inherited by F1 progeny through the germ cells. Subsequent and postnatal exposure of the F1 progeny to AEBN would immediately induce promotion followed by progression, leading to the observed acceleration of preneoplastic nodule appearance from the P to the F1 generation. Similarly, the germ cells of the F1 and F2 mice would inherit a promoting event, hence, the progressive advancement of period of preneoplastic nodule development from F1 to F2 generations and from F2 to F3. The significantly accelerated appearance of preneoplastic nodules is accompanied by extensive ultrastructural alterations (Figs. 1–7).

It can, thus, be concluded that AEBN induces extensive alteration and disruption of the ultrastructure of hepatocytes and the modulation in structure, especially of the mitochondria plays a vital role in allowing cells to evade apoptosis and survive despite cumulative damage due to prolonged exposure to AEBN. On transgenerational exposure to AEBN, the progressive increase in mitochondrial dysfunction exacerbates the consequence of concomitant loss of tumor-suppressor response, that is, loss of p53 function as reported earlier (Choudhury and Sharan, 2009), and loss of Brca1 and Brca2 function (Choudhury and Sharan, unpublished), thereby resulting in an increased predisposition to cancer in the transgenerationally exposed mice.

REFERENCES

Arismendi-Morillo GJ, Castellano-Ramirez AV. 2008. Ultrastructural mitochondrial pathology in human astrocytic tumors: potentials implications pro-therapeutics strategies. J Electron Microsc 57:33–39.

Boya P, González-Polo R, Casares N, Perfettini J, Dessen P, Larochette N, Métivier D, Meley D, Souquere S, Yoshimori T,

Pierron G, Codogno P, Kroemer G. 2005. Inhibition of macroautophagy triggers apoptosis. Mol Cell Biol 25:1025–1040.
Caruso RA, Fedele F, Finocchiaro G, Pizzi G, Nunnari M, Gitto G, Fabiano V, Rigoli L. 2008. Microvascular changes in human gastric carcinomas with coagulative necrosis: An ultrastructural study. Ultrastruct Pathol 32:184–188.
Chang MC, Ho YS, Lee PH, Chan CP, Lee JJ, Hahn LJ, Wang YJ, Jeng JH. 2001. Areca nut extract and arecoline induced the cell cycle arrest but not apoptosis of cultured oral KB epithelial cells: association of glutathione, reactive oxygen species and mitochondrial membrane potential. Carcinogenesis 22:1527–1535.
Choudhury Y, Sharan RN. 2009. Altered p53 response and enhanced transgenerational transmission of carcinogenic risk upon exposure of mice to betel nut. Environ Toxicol Pharmacol 27:127–138.
Dasgupta R, Saha I, Pal S, Bhattacharyya A, Gaurishankar SA, Nag TC, Das T, Maiti BR. 2006. Immunosuppression, hepatoxicity and depression of antioxidant status by arecoline in albino mice. Toxicology 227:94–104.
Degenhardt K, Mathew R, Beaudoin B, Bray K, Anderson D, Chen G, Mukherjee C, Shi Y, Gélinas C, Fan Y, Nelson DA, Jin S, White E. 2006. Autophagy promotes tumor cell survival and restricts necrosis, inflammation and tumorigenesis. Cancer Cell 10:51–64.
Gilkerson RW, Selker JM, Capaldi RA. 2003. The cristal membrane of mitochondria is the principal site of oxidative phosphorylation. FEBS Lett 546:355–358.
Hayat MA. 1985. Basic techniques for transmission electron microscopy. New York: Academic Press.
Hippert MM, O'Toole PS, Thorburn A. 2006. Autophagy in cancer: Good, Bad or Both. Cancer Res 66:9349–9351.
Lu S, Chang K, Liu C, Tseng Y, Lu H, Lee S, Lin S. 2006. Ripe areca nut extract induces G_1 phase arrests and senescence-associated phenotypes in normal human oral keratinocyte. Carcinogenesis 27:1273–1284.
Luciakova K, Kuzela S. 1992. Increased steady state levels of several mitochondrial and nuclear gene transcripts in rat hepatoma with a low content of mitochondria. Eur J Biochem 205:1187–1193.
Merkow LP, Epstein SM, Caito BJ, Bartus B. 1967. The cellular analysis of liver carcinogenesis: ultrastructural alterations within hyperplastic liver nodules induced by 2-fluorenylacetamide. Cancer Res 27:1712–1721.
Narama I, Imaida K, Iwata H, Nakae D, Nishikawa A, Harada T. 2003. A review of nomenclature and diagnostic criteria for proliferative lesions in the liver of rats by a working group of Japanese Society of Toxicologic Pathology. J Toxicol Pathol 16:1–17.
Nomura T. 1982. Parental exposure to X rays and chemicals induces heritable tumours and anomalies in mice. Nature 296:575–577.
Nomura T. 1983. X-ray induced germ-line mutation leading to tumors. Its manifestation in mice given urethane post-natally. Mutat Res 121:59–65.
Paul MK, Mukhopadhyay AK. 2007. Cancer-the mitochondrial connection. Biologia Bratislava 62:371–380.
Raick AN. 1973. Ultrastructural, histological, and biochemical alterations produced by 12-*o*-tetradecanoyl-phorbol-13-acetate on mouse epidermis and their relevance to skin tumor promotion. Cancer Res 33:269–286.
Saha I, Chatterji U, Chaushuri-Sengupta S, Nag TC, Nag D, Banerjee S, Maiti BR. 2007. Ultrastructural and hormonal changes in pineal-testicular axis following arecoline administration in rats. J Exp Zool Part A Ecol Genet Physiol 307A:187–198.
Sharan RN. 1996. Association of betel nut with carcinogenesis. Cancer J 9:13–19.
Shiraishi H, Okamoto H, Yoshimura A, Yoshida H. 2006. ER-stress induced apoptosis and caspase-12 activation occurs downstream of mitochondrial apoptosis involving Apaf-1. J Cell Sci 119:3958–3966.
Sundqvist K, Liu Y, Nair J, Bartsch H, Arvidson K, Grafström RC. 1989. Cytotoxic and genotoxic effects of areca nut-related compounds in cultured human buccal epithelial cells. Cancer Res 49:5294–5298.
Terzakis JA. 1968. Uranyl acetate a stain and a fixative. J Ultrastruct Res 22:168–184.
Tomatis L, Narod S, Yamasaki H. 1992. Transgeneration transmission of carcinogenic risk. Carcinogenesis 13:145–151.
Wary KK, Sharan RN. 1988. Aqueous extract of betel-nut of North-East India induces DNA strand breaks and enhances rate of cell proliferation in vitro. J Cancer Res Clin Oncol 114:579–582.
Zamaraeva MV, Sabirov RZ, Maeno E, Ando-Akatsuka Y, Bessonova SV, Okada Y. 2005. Cells die with increased cytosolic ATP during apoptosis: a bioluminescence study with intracellular luciferase. Cell Death Differ 12:1390–1397.
Zhang XH, Takenaka I. 1995. Interstitial stroma and carcinogenesis: ultrastructural observations in rat bladder treated with *N*-butyl-*N*-(4-hydroxybutyl) nitrosamine. Urol Res 24:177–181.
Zink D, Fischer AH, Nickerson JA. 2004. Nuclear structure in cancer cells. Nat Rev Cancer 4:677–687.